Journal of the European Ceramic Society **16** (1996) 1089–1098

PII: S0955-2219(96)00024-6
0955-2219/96/$15.00

Phase Equilibrium Relationships in the System Al_2O_3–TiO_2–MnO, Relevant to the Low-Temperature Sintering of Alumina

M. C. Moreira & A. M. Segadães*

Departamento de Engenharia Cerâmica e do Vidro, Universidade de Aveiro, 3180 Aveiro, Portugal

(Received 20 September 1994; revised version received 4 January 1996; accepted 8 January 1996)

Abstract

A great deal of research work has been devoted to lowering the sintering temperature of ceramic powders of varied nature, to fulfil a variety of purposes. Both experimentation and theory show that the sintering temperature of alumina can be lowered to 1400°C and below by using small particle sizes and certain additives like TiO_2 and/or MnO. The general idea is that sintering is aided by the development of a liquid phase at this low temperature, due to the presence of the additives. However, there is no phase diagram available to throw light on this matter. For this reason, the present work was aimed at investigating the phase equilibrium relationships in the ternary, non-condensed system Al_2O_3–TiO_2–MnO, in air.

Selected compositions in this system were prepared from reagent-grade oxides, uniaxially pressed into 6 mm cylindrical pellets, fired at temperatures between 1000 and 1650°C for 2 to 22 h, water-quenched, and observed by X-ray diffraction and scanning electron microscopy, the composition of some of the phases identified being evaluated by energy-dispersive spectroscopy. These experiments led to the definition of the compatibility triangles and a tentative location of the boundary curves between primary phase fields is presented. © *1996 Elsevier Science Limited.*

1 Introduction

To aid the sintering process, i.e. to sinter faster or at lower temperatures, the reactivity of the particles to be sintered must be increased. In other words, finer grain sizes are needed. This effect is well documented in the literature, for a variety of systems. However, in those cases in which the properties of the sintered body are not unduly reduced by the use of sintering aids, this is still the easiest way of lowering the sintering temperature. These aids promote sintering either by causing the development of solid solutions and lattice defects, or the development of a liquid phase, both favouring the diffusion processes necessary to sintering.

A number of researchers have studied the effect of various additives on the densification of non-reactive alumina powders, based on the liquid-phase mechanism.[1–3] The general conclusion is that there is an optimum amount of each additive at a given temperature to reach maximum density and, the higher the temperature, the smaller the amount of additive needed. With a liquid phase present at high temperatures, the resulting sintered alumina bodies are not adequate for structural applications. But alumina is still the ideal material for cold abrasion/erosion applications (e.g. thread guides, spray nozzles), where it is important to be able to sinter at lower temperatures. In these cases, the high-temperature liquid phase can even enhance the cold mechanical strength, an indirect measure of the abrasion resistance of the ceramic body.

The work of Cutler *et al.*[1] on the effect of additions of manganese, copper and titanium oxides on the sintering behaviour of alumina, showed that combinations of manganese and titanium oxides were the most effective in lowering the sintering temperature, especially when present in equal amounts. The authors detected the presence of a liquid phase and found that minimum grain growth occurred for 3–4% mixed additive, sintered between 1300 and 1400°C, the resulting ceramic having reached densities of the order of 3·80 g cm.$^{-3}$ More recently, Filbri *et al.*[3] investigated this same system from a different perspective, since they were trying to sinter high alumina compositions without a significant reduction in porosity. The authors kept the total amount of additives very low (≤ 0·5%), to stay close to the solid solubility limits (although there is no consensus on this value) and avoid the development of a liquid phase.

*To whom correspondence should be addressed.

Research work such as this would be much easier if the phase diagram of the system Al_2O_3–TiO_2–MnO_2–MnO was available. This system is a non-condensed one, in which the phase stability is determined not only by the temperature and composition but also by the oxygen partial pressure in the gaseous phase. In air, it was observed[4] that the evolution of oxygen as the temperature rises is not easily reversed on cooling. In other words, the high-temperature reduced forms tend to be retained at lower temperatures. This will be more the case when other components are present, with which the reduced oxide can react. Therefore, the phase equilibrium relationships in the system Al_2O_3–TiO_2–MnO_2–MnO can be approximated by those for the Al_2O_3–TiO_2–MnO system at temperatures above 800°C.

In the literature, only the isobaric phase diagrams of the binary systems are available,[5] albeit old. Four binary compounds are reported, namely $Al_2O_3.TiO_2$ (AT), $MnO.Al_2O_3$ (MA), $MnO.TiO_2$ (MT) and $2MnO.TiO_2$ (M_2T). If no ternary compounds are formed within the system, its phase diagram should contain five solid-phase compatibility triangles and the corresponding five invariant points. The present work was aimed at investigating the phase equilibrium relationships in the ternary, non-condensed system Al_2O_3–TiO_2–MnO in air, and tentatively locating the position of the invariant points.

2 Experimental Procedure

In the present work, selected compositions were prepared from BDH alumina powder (chromatography), after dry grinding in a planetary mill for 30 min, TiO_2 (Merck) and MnO_2 (Merck) powders, all sieved through 43 μm (325 mesh).

Prior to any experiments, the mineralogy of the starting powders was confirmed by X-ray diffraction (XRD; using Cu K_α radiation). Moreover, the oxidation behaviour of the manganese oxide, kept dry in sealed containers, was investigated by thermogravimetric analysis (TGA) using a Stanton Redcroft thermobalance with a 2°C min^{-1} heating (and cooling) rate, up to 1200°C.

The appropriate amounts of the reactants were dry-mixed for 30 min in a Glen-Creston mixer–miller, and uniaxially dry-pressed into 6 mm cylindrical pellets using a hard-steel die under a pressure of ~50 MPa. Each pellet was then wrapped in platinum foil, lowered into the furnace held at the chosen soaking temperature (SiC vertical tube furnace for temperatures up to 1450°C or a molybdenum-wound vertical tube furnace for higher temperatures), kept at that temperature for 2 to 22 h, and water-quenched. Temperatures were measured with Pt/Pt–13% thermocouples.

To guarantee that equilibrium had been established, particularly in those samples fired at lower temperatures, the same composition was held for successively longer times at the particular temperature, until the phase assemblage observed did not change any further. The shortest time required to attain this was then considered to be enough to establish the equilibrium state. Naturally, samples fired at higher temperatures, most of which contained a liquid phase, needed shorter firing times.

The fired samples were then prepared for X-ray powder diffraction and/or scanning electron microscopy (SEM) analysis (Jeol JSM-35C) on epoxy-mounted polished surfaces. Different phases present different morphologies and colours, to each of which a typical composition could be indexed by semi-quantitative energy-dispersive spectrometer (EDS) analysis (Tracor TN 2000). Sample charging in SEM and EDS was prevented by carbon coating. EDS was carried out using elemental standards, the oxygen being calculated by difference.

Table 1 gathers the relevant data so obtained, after correcting the compositions for the corresponding oxygen loss. This table is constructed in the usual way for phase equilibrium studies in ceramic oxide systems,[6] i.e. only the major phases present are listed, those present in only trace amounts, or when they do not represent true equilibrium, being shown in parentheses. Sometimes, due to the poorly defined microstructure, some details could not be determined unambiguously during microscopic examination. In these cases the particular phase assemblage is listed as 'poor microstructure'.

3 Results and Discussion

3.1 Oxidation behaviour of manganese oxide

Although alumina and titania are stable oxides in air, even at high temperatures, in the Mn–O system the oxides MNO_2, Mn_2O_3, Mn_3O_4 and MnO exist as stable phases that can interconvert depending on the temperature and the oxygen partial pressure. The reactions between the condensed phases and the oxygen of the gaseous phase in such metal–oxygen systems can easily be investigated by TGA, where the oxygen evolution caused by the temperature rise translates into directly recordable weight loss. In the binary systems like Mn–O, it is particularly helpful to convert the weight loss curves into dissociation curves, plotting the remaining oxygen/initial metal molar ratio, O/Mn, against temperature.

Figure 1(A) shows the weight loss curve obtained in air from a sample of manganese oxide initially weighing 354·8 mg. As can be observed, there is an initial, small, slow weight loss corresponding to the change in oxygen stoichiometry as the isobar

Table 1. Selected compositions and phases identified in the system Al_2O_3–TiO_2–MnO (A = alumina; T = titania; M = manganesia)

Composition (wt%)			*Temp*	*Time*	*Phase identified*
Al_2O_3	*MnO*	*TiO_2*	*(°C)*	*(h)*	*(SEM)*
65·00	30·00	5·00	1457	4	MA+A+liquid
	(1)		1496	2	MA+A+liquid
			1600	4	MA+A+liquid
65·00	25·00	10·00	1300	18	MA+A+liquid
			1342	4	MA+A+liquid
			1386	4	MA+A+liquid
	(2)		1447	4	MA+A+liquid
			1496	2	MA+A+liquid
65·00	17·00	18·00	1250	16	A+MT+liquid
			1342	4	A(+MT)+liquid
			1396	19	A+liquid
	(3)		1447	4	A(+MT)+liquid
			1496	2	A+liquid
65·00	10·00	25·00	1335	4	Poor microstructure
			1378	4	Poor microstructure
	(4)		1447	4	A+AT+liquid
			1600	4	A+liquid
49·00	46·00	5·00	1100	22	MA+MT+liquid
	(5)		1200	12	MA(+MT)+liquid
			1300	19	MA+liquid
40·00	55·00	5·00	1290	10	MA(+T)+liquid
			1340	4	MA+liquid
			1381	4	MA+liquid
	(6)		1446	4	MA+liquid
			1535	2	MA(+T)+liquid
40·00	45·00	15·00	1100	22	MA+MT+liquid
			1340	4	MA(+MT)+liquid
	(7)		1381	4	MA(+MT)+liquid
			1457	4	MA+liquid
			1535	2	liquid(+MA)
40·00	35·00	25·00	1030	19	Poor microstructure
			1208	11	MT+MA+A(+liquid)
			1250	16	MT+MA(+A)+liquid
	(8)		1290	10	MT+MA(+A)+liquid
			1320	17	MT(+A)+liquid
			1400	4	Abundant liquid
40·00	20·00	40·00	1340	4	MT(+A)+AT+liquid
	(9)				
40·00	5·00	55·00	1342	4	AT+T(+A)+liquid
	(10)		1446	4	AT+T+liquid
			1650	6	AT+liquid
20·00	62·50	17·50	1100	22	MT+M_2T+liquid
	(11)				
20·00	54·00	26·00	1035	16	Poor microstructure
			1098	4	MT+MA+liquid
			1210	$7^{2/3}$	MT+MA+liquid
	(12)		1250	16	MT+MA+liquid
			1300	12	Abundant liquid
20·00	43·00	37·00	1035	16	Poor microstructure
			1098	19	Poor microstructure
			1210	$7^{2/3}$	Poor microstructure
	(13)		1250	19	MT+MA+liquid
			1300	18	MT+abundant liquid
			1380	16	Abundant liquid
20·00	20·00	60·00	1100	4	Poor microstructure
			1126	5	Poor microstructure
	(14)		1210	$7^{2/3}$	MT+AT+liquid
			1252	19	MT+AT+liquid
10·00	85·00	5·00	1200	12	M(+T)+MA+liquid
	(15)		1300	12	M(+T)+liquid
			1380	16	M(+T)+liquid
10·00	55·00	35·00	990	12	Poor microstructure
			1126	5	MT+MA(+A)+ab.liquid
	(16)		1252	19	MT+M_2T+liquid
			1290	11	MT+M_2T+liquid
10·00	5·00	85·00	1300	12	T+AT+liquid
	(17)				

traverses the dioxide single-phase field. At constant pressure, isothermal weight losses, corresponding to sharp changes in the O/Mn molar ratio, describe the isobaric invariant equilibrium between two condensed phases. Such a sharp change can be observed at ≈630°C, which corresponds to the invariant equilibrium between the original 'MnO_2' and non-stoichiometric Mn_2O_3. Up to ≈725°C a gradual conversion to Mn_3O_4 occurs, suggesting that there is a region of continuous mutual solid solubility between the sesquioxide and the spinel instead of invariant equilibrium between the two phases. This is followed by a second gradual conversion of the spinel to MnO, which is complete at ≈800°C. Above this temperature MNO is the stable oxide, showing clear oxygen deficiency above 960°C. Assuming that the O/Mn molar ratio at ≈800°C is unity, then, by working backwards, it is possible to calculate the oxygen stoichiometry in the starting manganese oxide and plot a corrected O/Mn molar ratio vs. temperature curve, as shown in Fig. 1(B). It is known that commercial 'MnO_2' varies from $MNO_{1.98}$ to $MnO_{1.75}$, and the starting oxide was found to be $MnO_{1.94}$.

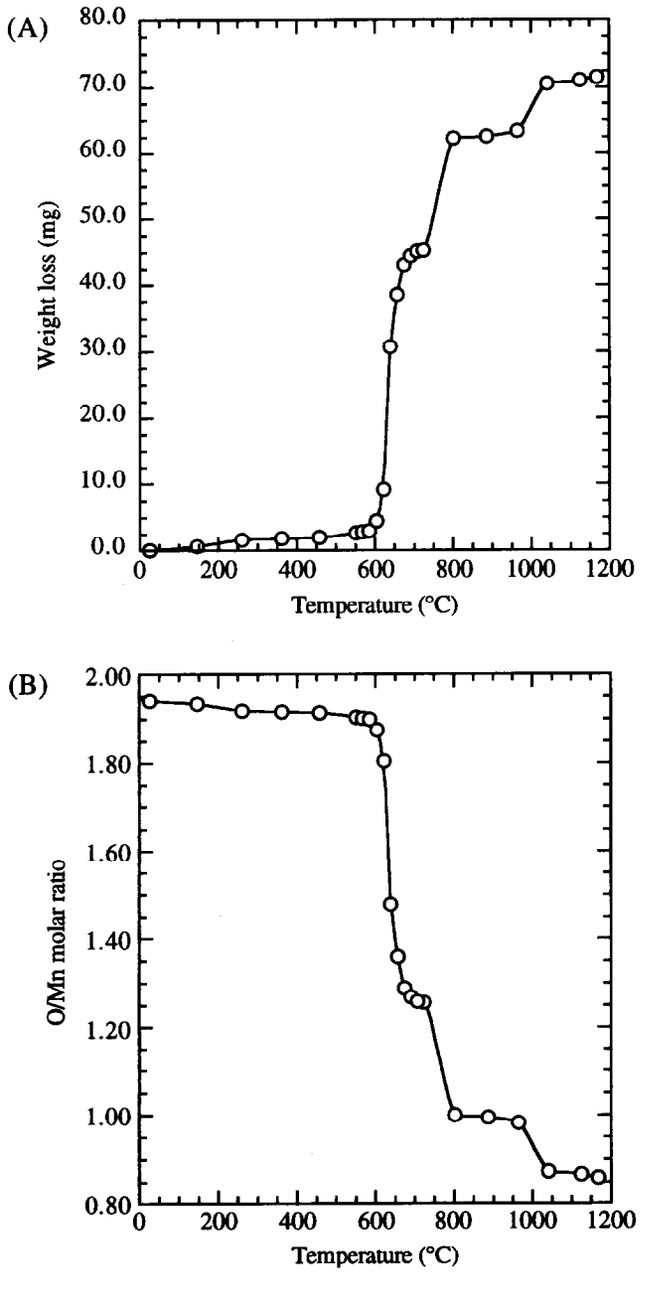

Fig. 1. TGA curves obtained for 354·8 mg of original MnO_2: (A) weight loss curve, and (B) corrected dissociation curve.

The difficulty in reversing the oxygen loss became apparent when no significant weight gain was recorded upon cooling. This was confirmed by X-ray diffraction of the powder after TGA, which showed only MnO and Mn_2O_3 (no MnO_2) peaks.

In the light of these findings, it is valid to approximate the phase equilibrium relationships in the system Al_2O_3–TiO_2–MnO_2–MnO to those for the Al_2O_3–TiO_2–MnO system at temperatures above 800°C.

3.2 Choice of the solid-phase compatibility triangles

Only the isobaric phase diagrams of the binary systems are available in the literature[5] and four binary compounds are reported: $Al_2O_3.TiO_2$ (AT), $MnO.Al_2O_3$ (MA), $MnO.TiO_2$ (MT) and $2MnO.TiO_2$ (M_2T). Of these, only MT shows incongruent melting behaviour. As for AT, there has been a recent resurgence of interest in this material due to radical improvements in microstructural control allied to its excellent thermal properties. Its successful application relies on the ability to control the microcracking phenomenon and understand the decomposition behaviour. Even though considerable work has been carried out to explain the mechanism of decomposition and the effect of additives on such behaviour, the important fact remains that AT is unstable below ≈1200°C.[7–9]

As described elsewhere,[10] preliminary work was carried out to investigate which were the compatibility triangles in the system. If no ternary compounds are formed within the system, its phase diagram should contain five solid-phase compatibility triangles (which can be arranged in seven alternative ways) and the corresponding five invariant points. A set of carefully chosen compositions was fired between 1100 and 1400°C for 4 to 7 h, to establish equilibrium, and slow-cooled to ambient temperature. Powder X-ray diffraction analysis carried out on these samples showed that no ternary compounds are indeed formed within the system and that the solid-phase compatibility triangles are set as shown in Fig. 2 (AT room-temperature instability is accounted for by showing the AT-MT tie-line as a dashed line).

3.3. Microstructure analysis of selected compositions

In all the samples, and when present, the titania grains appear as rounded white crystals [Fig. 3(A)]; alumina is always very dark grey (almost black) and

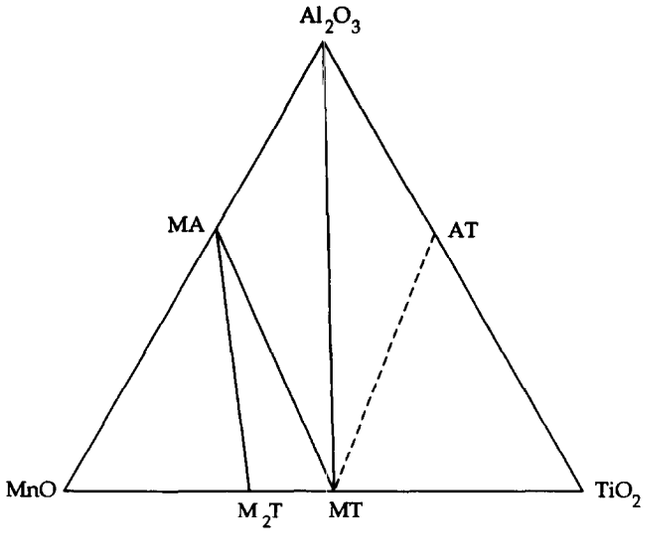

Fig. 2. Layout of solid-phase compatibility triangles[10] (AT room-temperature instability is accounted for by showing the AT–MT tie-line as a dashed line).

appears either as well developed long polygonal grains [Fig. 3(B)] or smaller round ones; AT crystals are also polygonal, but of a lighter grey [Figs 3(A), (B)]; MT grains show up with smooth contours and are very light grey [Figs 3(B), (C)] whereas MA grains are long, smooth and medium grey [Fig. 3(C)]. M crystals are polygonal and light grey. The M_2T phase is rather hard to pick up and usually appears as grey areas associated with T and/or MT grains. The intergranular phase of various greys (lighter in the alumina-rich compositions, darker in the manganesia-rich ones) is the liquid (glass) phase. Black spots are pores.

Samples frequently appear profusely cracked, particularly the glassy phase, due to the thermal shock during quenching. It was found that the liquid phase sometimes devitrifies during quenching, with crystallization of dendrites. Also, unreacted alumina and/or titania grains can sometimes be found. Such non-equilibrium phases, readily identified in the microstructure, are placed in parentheses in Table 1.

3.4 Tentative phase diagram for the system Al_2O_3–TiO_2–MnO

The first working hypothesis assumed during this investigation was that the MT phase would keep it perithetic behaviour inside the ternary system. That was never contradicted by the experimental data obtained. Then, the location and character of

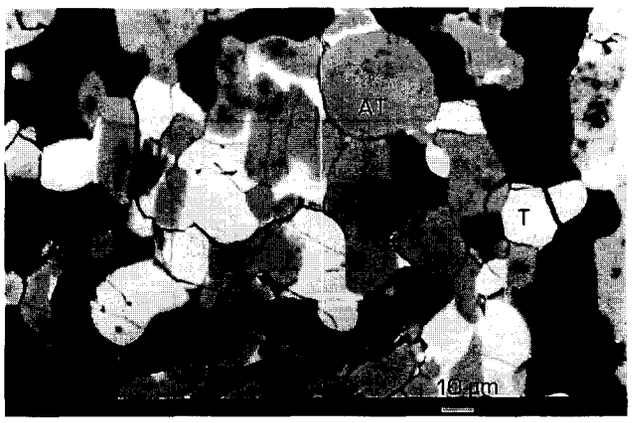

(A)

(B)

(C)

Fig. 3. Representative microstructures observed in the samples investigated: (A) 40 Al_2O_3 + 55 TiO_2 + 5 MnO, at 1342°C showing titania grains (white) and AT grains (grey), thermal shock cracks, liquid films and pores (black). (B) 40 Al_2O_3 + 40 TiO_2 + 20 MnO, at 1340°C, showing one unreacted alumina crystal (very dark grey), AT grains (grey), MT grains (light grey), a patch of devitrified liquid phase and extensive thermal shock cracks. (C) 20 Al_2O_3 + 26 TiO_2 + 54 MnO, at 1250°C, showing MA grains (medium grey), MT grains (light grey) and intergranular liquid films.

A1

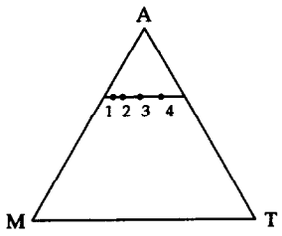

Key to symbols

- ○ Liquid (L)
- ▣ A+L
- × M+L
- \+ MA+L
- ◐ AT+L
- ▣ MT+L
- ⊕ M+MA+L
- ◇ A+MA+l
- □ A+AT+L
- ▲ A+MT+L
- ⌀ MA+MT+L
- △ AT+MT+L
- ◒ T+AT+L
- ▽ MT+M_2T+L
- ■ A+MA+MT
- ● poor microstructure

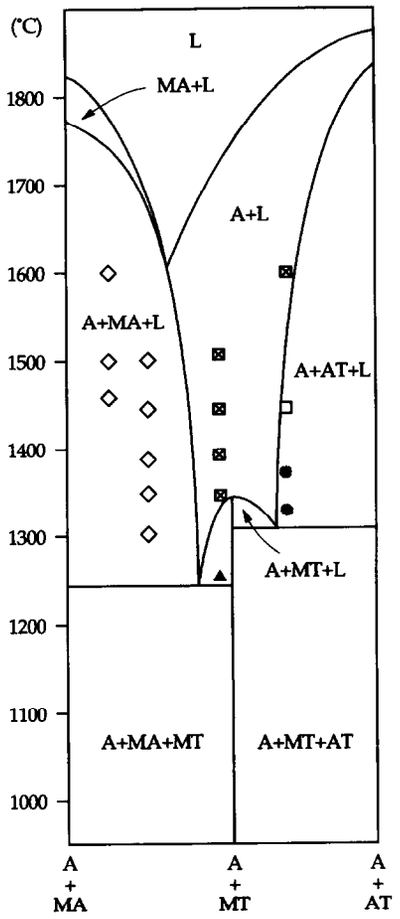

A2

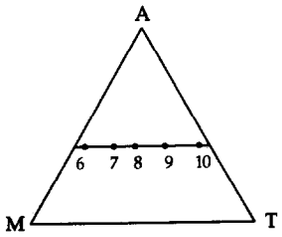

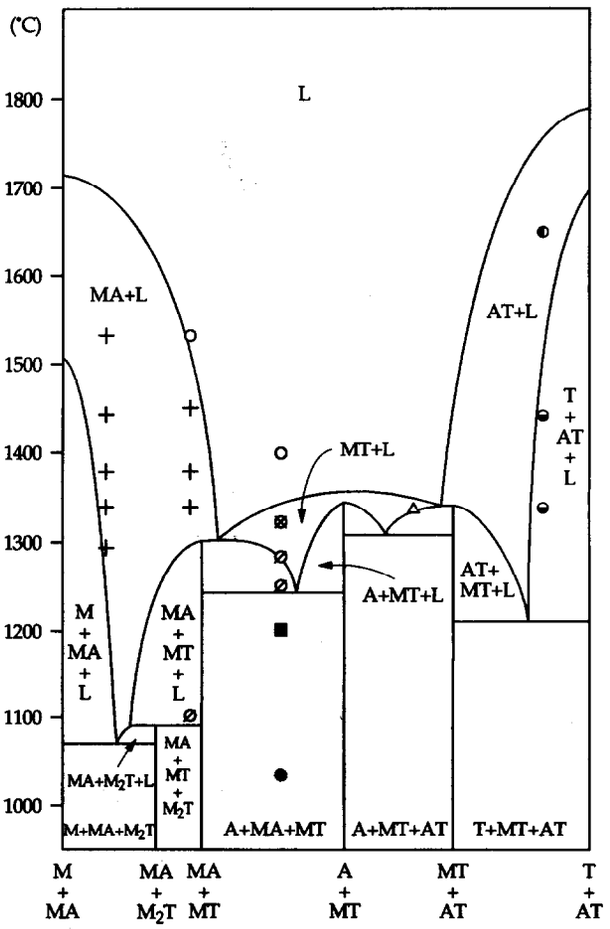

Fig. 4. Isoplethal sections: (A) at constant 65 and 40 wt% Al_2O_3 and key to symbols, (B) at constant 20 and 10 wt% Al_2O_3 and (C) at constant 5 wt% TiO_2 and 5 wt% MnO.

B1

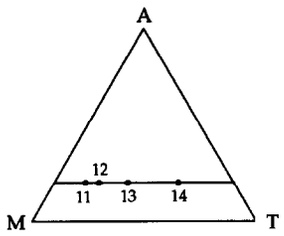

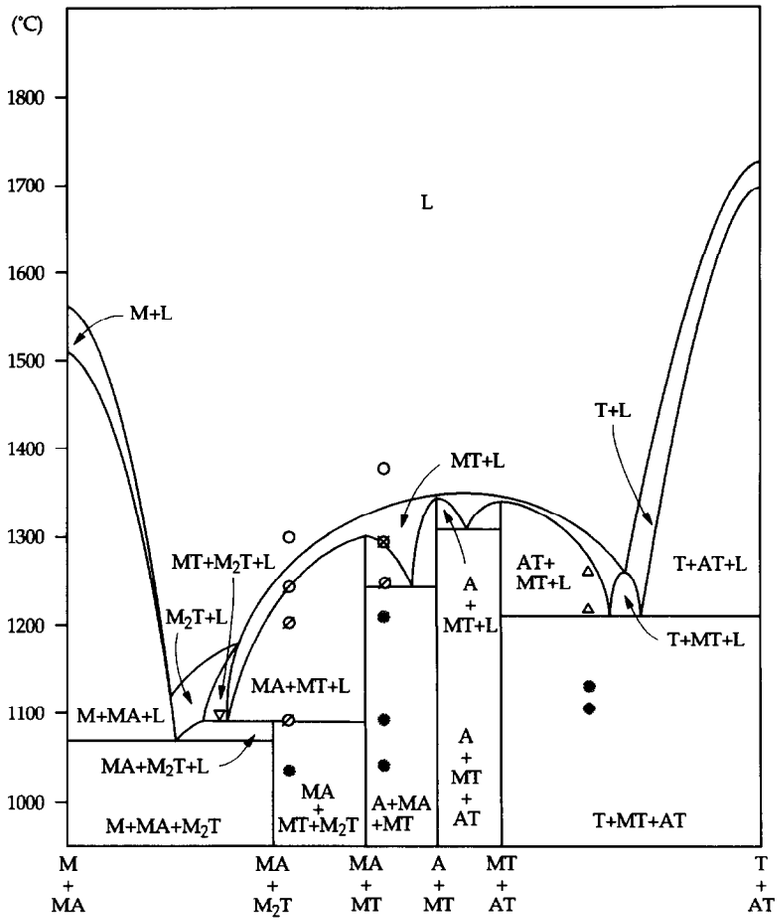

B2

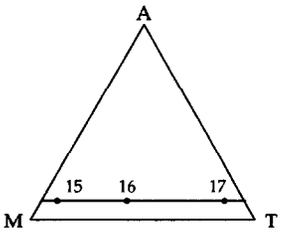

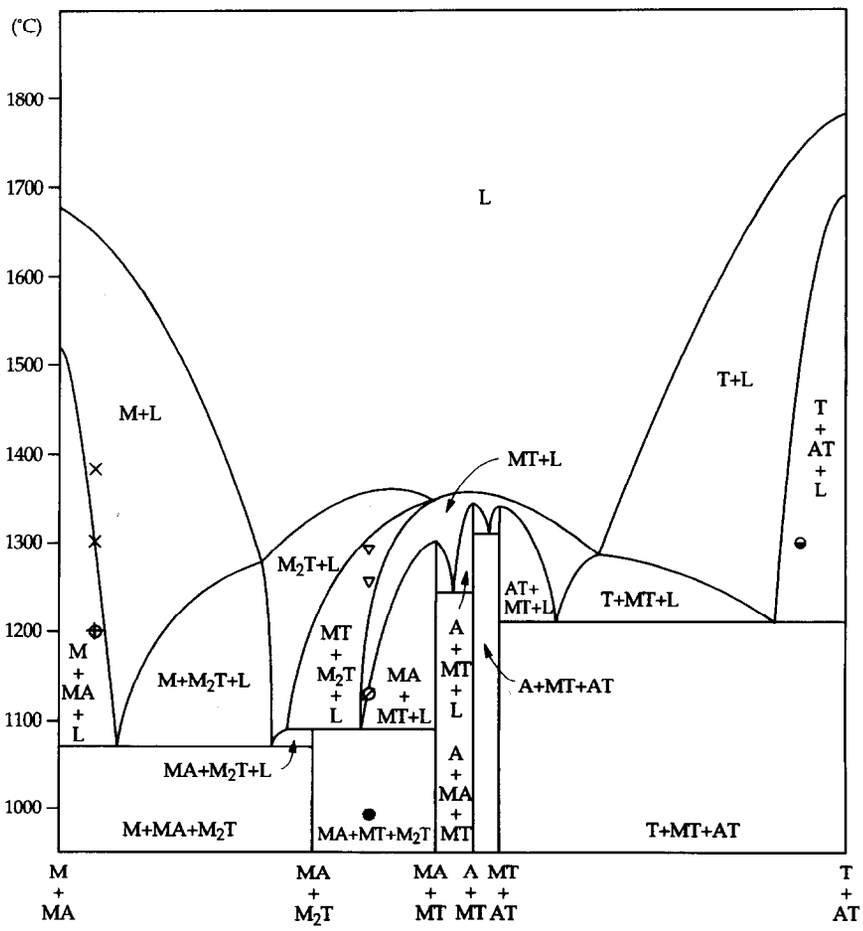

Fig. 4. Continued

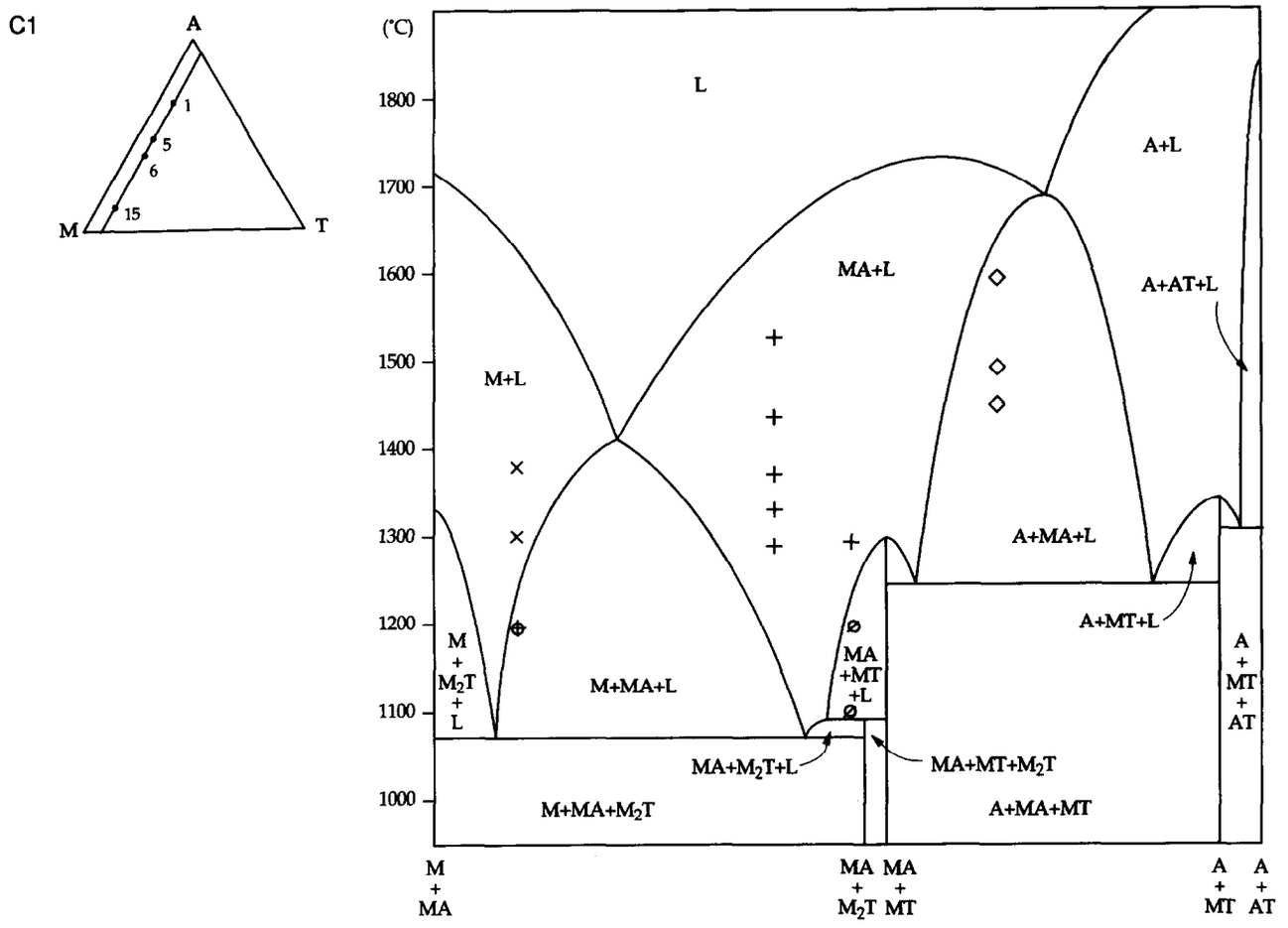

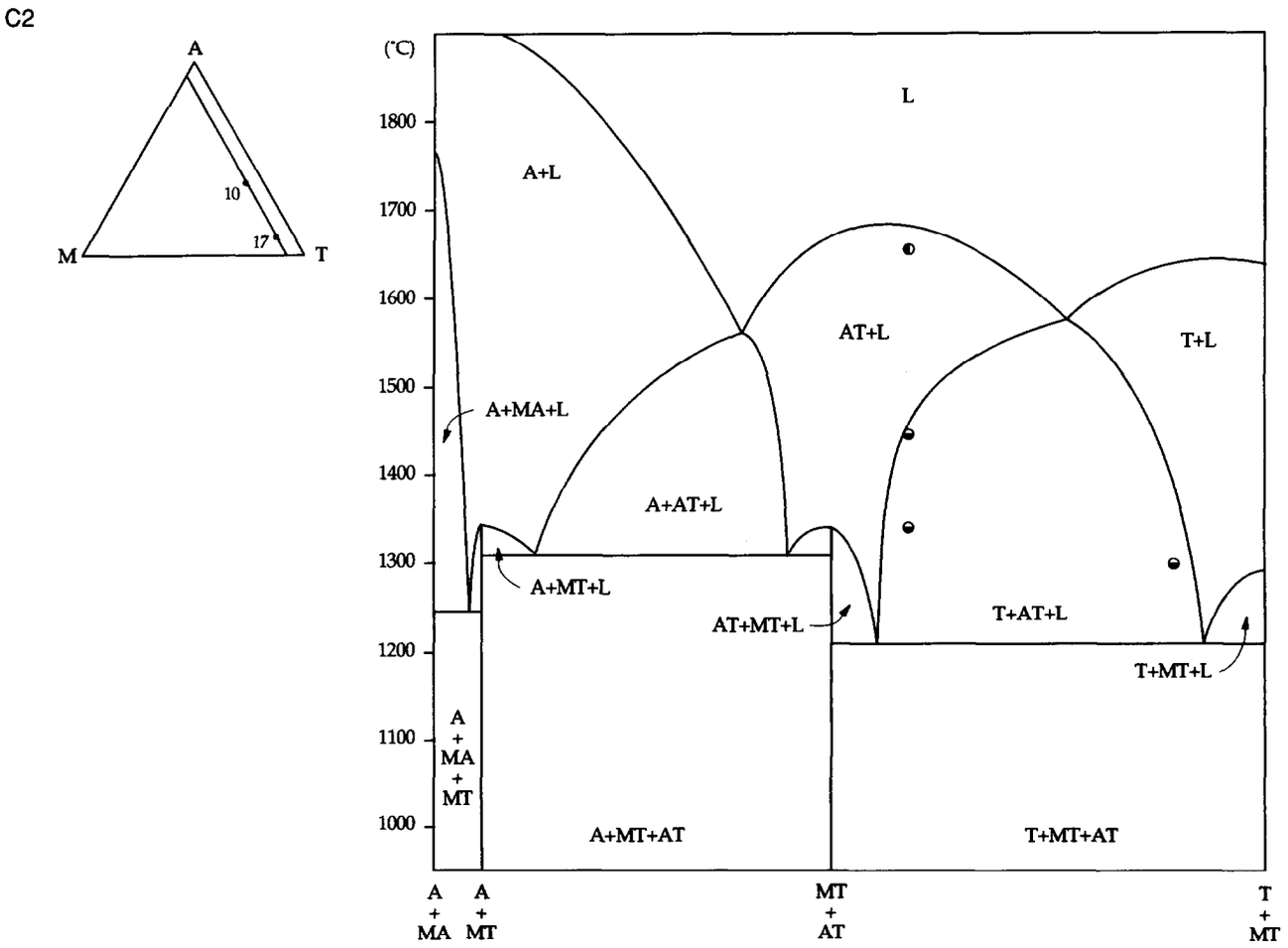

Fig. 4. Continued

the ternary invariant points had to be chosen and worked with. For each of these working hypotheses, isoplethal sections similar to those in Fig. 4 were constructed. When a conflict between the phase fields in the isoplethal sections and the experimental data was found, the location and/or character of the ternary invariant points (and the boundary lines connecting them) was changed in order to resolve the conflict. Several such iterations were needed until the final version of the isoplethal sections, presented in Fig. 4, was reached.

From them and the relevant information extracted from the binary systems,[5] Fig. 5 was constructed. Shown in the diagram are the composition points mentioned in Table 1 and the corresponding primary crystallization paths. In this diagram, the location of all the liquid isotherms and the invariant points are but educated guesses, to suit the experimental results obtained.

4 Implications for the Low-Temperature Sintering of Alumina

The ternary system Al_2O_3–TiO_2–MnO is a rather good example of how the combination of three refractory components can produce low-temperature liquid phases. From the three binary systems that compose the ternary Al_2O_3–TiO_2–MnO, only the liquid phases in the binary TiO_2–MnO can be considered as low-temperature ones. Thus, any low-temperature liquidus region within the ternary was expected to lie close to this binary. What could not have been guessed was the extension (and flatness) of the low-temperature liquidus plateau at about 1300°C, occupying most of the central region of the ternary, bordered by sharp rising liquidus surfaces towards the high-temperature binaries Al_2O_3–MnO and Al_2O_3–TiO_2. In fact, the results of the present work suggest that there might be a scant 100°C decrease in liquidus temperature over a composition range of roughly 40% in alumina.

Given the low solid solubility of TiO_2 and MnO in alumina reported by various authors, particularly at low temperatures,[3] the sintering-aid effect of these oxides would mostly be accomplished by a liquid-phase mechanism, noticeable at temperatures above 1300°C. Since the low-temperature liquidus plateau is roughly circular and located almost symmetrically in relation to the Al_2O_3–MnO and Al_2O_3–TiO_2 binaries, it is no surprise that equal amounts of manganese and titanium oxides are the most effective combination in lowering the sintering temperature of alumina. Also, the amount of liquid phase

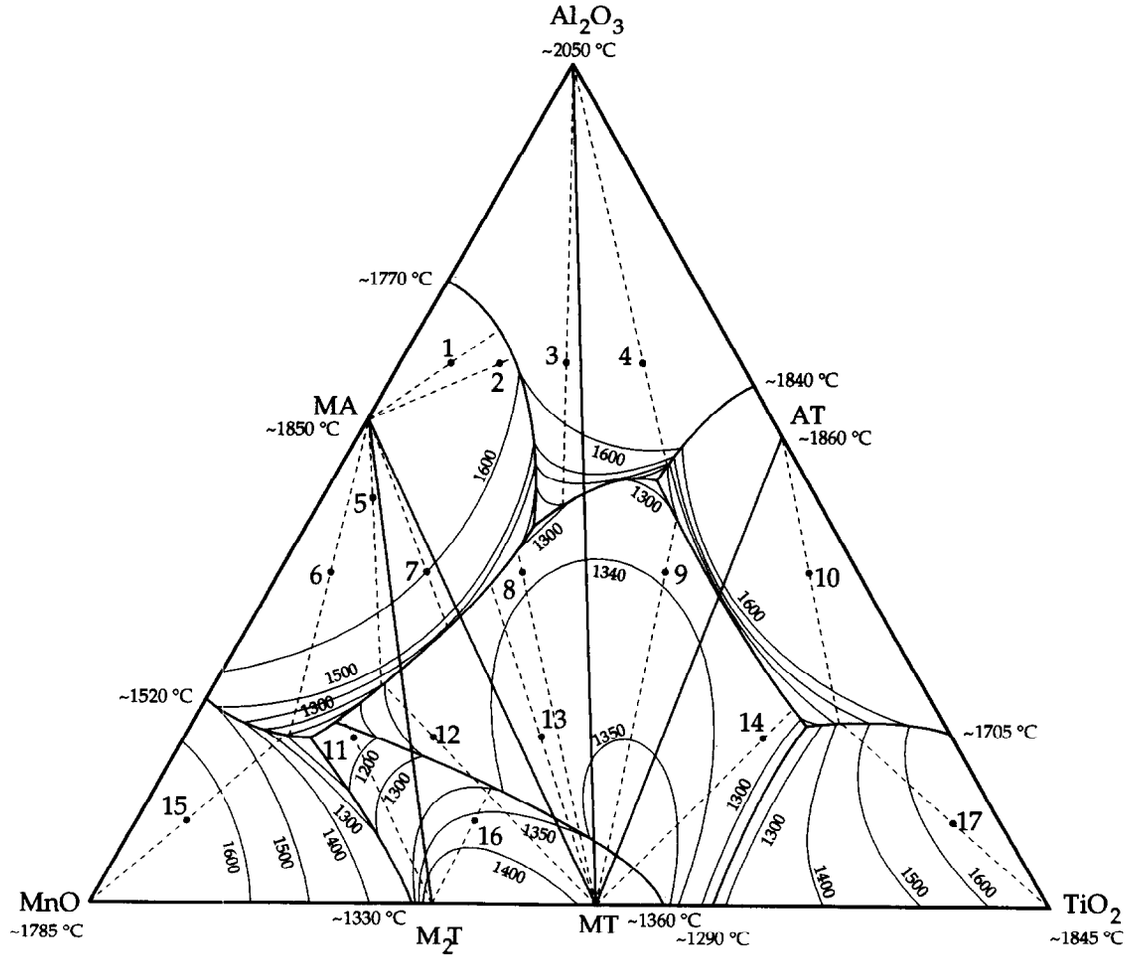

Fig. 5. Tentative phase diagram for the system Al_2O_3–TiO_2–MnO. The locations of all the liquid isotherms and the invariant points are but educated guesses, to suit the information extracted from the binary systems[5] and the experimental results obtained.

formed depends on the proximity of the eutectic valley to the alumina corner: the closer the valley, the larger the amount of liquid. This explains why that particular combination is an effective sintering aid even when present in such small amounts.

Another feature to note is the steepness of the liquidus surface towards the alumina corner and away from the central region. This implies that the quantity of liquid needed to aid sintering can be chosen carefully by selecting the correct composition; the quantity of liquid will then be relatively constant for a wide span of temperatures. This gives a highly convenient system from the point of view of manufacturing in precisely the same way that the liquid immiscibility plateau in the lime–silica system explains the special aptitude of lime as additive in the manufacture of silica bricks or that the silica viscosity makes the manufacturing of porcelains relatively forgiving. A quick calculation using the lever rule shows that 4% of the mixed oxides produce a quantity of liquid that varies very little with temperature, as shown below:

Temperature(°C)	1200	1250	1300	1400	1500
%Liquid phase	6·3	7·0	7·2	7·7	7·9

5 Conclusions

Earlier research work[1–3] showed that non-reactive alumina powders could be sintered at temperatures below 1400°C using combinations of titanium and manganese oxides as sintering aids. Phase equilibrium research work carried out with selected compositions in the system Al_2O_3–TiO_2–MnO, in air, led to the construction of a plausible version of its phase diagram. The tentative diagram shows that in the composition range for low-temperature sinterable aluminas (containing sintering aids), initial melting occurs below 1300°C and sintering is assisted by a liquid phase as proposed by the earlier authors. In this diagram, the location of the liquid isotherms and the invariant points are educated guesses and extensive experimental work would be needed to establish their exact location.

Acknowledgements

The authors wish to thank C. M. Sá from CEMUP, Portugal, for the SEM work carried out. The present work was partially funded by INIC, Portugal.

References

1. Cutler, I. B., Bradshaw, C., Christensen, C. J. & Hyatt, E. P., Sintering of alumina at temperatures of 1400°C and below. *J. Am. Ceram. Soc.*, **40**[4] (1957) 134–139.
2. Kostic, E., Kis, S. & Boskovic, S., Liquid phase sintering of alumina. *Powder Metall. Int.*, **19**[4] (1987) 41–43.
3. Filbri, J. W., Schram, H. L. & Sinnema, S., Sintering of porous alumina using MnO and TiO_2. In *Fourth EURO CERAMICS, Vol. 2*, ed. C. Galassi. Faenza Editrice SpA, 1995, pp., 257–264.
4. Oliveira, V. A. G. & Brett, N. H., Phase equilibria in the system MgO–Mn_2O_3–MnO–$CaSiO_3$ in air. *J. de Phys.*, **47**[2] (1986) Cl–453–459.
5. Levin, E. M., Robbins, C. R. & McMurdie, H. F., In *Phase Diagrams for Ceramists*, ed. M. K. Reser. The American Ceramic Soc., Columbus, OH, 1974, Figs 277, 316 and 4376.
6. Greca, M. C., Emiliano, J. V. & Segadães, A. M., Revised phase equilibrium relationships in the system Al_2O_3–ZrO_2–SiO_2. *J. Eur. Ceram. Soc.*, **9** (1992) 271–283.
7. Thomas, H. A. J. & Stevens, R., Aluminium titanate—a literature review, Part 1: Microcracking phenomena. *Br. Ceram. Trans. J.*, **88** (1989) 144–151.
8. Thomas, H. A. J. & Stevens, R., Aluminium titanate —a literature review, Part 2: Engineering properties and thermal stability. *Br. Ceram. Trans. J.*, **88** (1989) 184–190.
9. Thomas, H. A. J. & Stevens, R., Aluminium titanate —a literature review, Part 3: Preparation of powders. *Br. Ceram. Trans. J.*, **88** (1989) 229–233.
10. Moreira, M. C., Segadães, A. M., Salvini, V., Mariano, W. A. & Morelli, M. R., Relações de compatibilidade no sistema Al_2O_3–TiO_2–MnO e a sua relevância na sinterização da alumina baixas temperaturas. *Cerâmica (São Paulo)*, **34**[227] (1988) 184–188.